

Supporting information

Experimental procedures

Preparation of TiO₂ nanorod arrays. TiO₂ nanorods were grown on fluorine doped tin oxide (FTO) by a solvothermal approach. In detail, prior to the synthesis, FTO glass was washed by acetone and water for several times, and dried by blowing with nitrogen flow. The clean substrates were placed in Teflon reactor (50 mL), containing 15 mL of DI water, 13 ml hydrochloric acid and 0.30 ml tetrabutyl titanate. The Teflon reactor was sealed in a stainless-steel jacket, and it was kept in an electric oven at 150°C for 12 hours. The reactor cooled down to ambient condition. The as-grown TiO₂ nanorods were obtained on FTO glasses. The as-prepared TiO₂ photoanode was obtained by washing with deionized (DI) water and annealed in air at 550 °C for an hour. Nitrogen doped TiO₂ (N:TiO₂) nanorods were prepared by annealing the pristine TiO₂ nanorods in ammonia atmosphere in vacuum furnace at 550°C for 2 hours, and the prepared N:TiO₂ nanorods presented yellow feature.

Coating TCN films on TiO₂ nanorod arrays. Urea and 2,4,6-tris(4-bromophenyl)-1,3,5-triazine were homogeneously mixed in a weight ratio of 1:0.003 as precursor to coat co-polymerized TCN films on TiO₂ nanorods. In detail, as-prepared TiO₂ photoanode was buried into the precursor, in a crucible. The crucible was annealed at 500 °C with rate of 3 °C/mins, and the annealing temperature is maintained for 4 hours. The as prepared samples cooled down to ambient conditions. The photoanodes were obtained by washing with DI water. Typical polymeric carbon nitride (PCN) coated TiO₂ nanorod arrays were prepared by same procedure by replacing a mixed precursor with using pristine urea.

Preparation of cathode. The Cu mesh was used as cathode, it was prepared by firstly washing with hydrochloric acid solution to remove copper oxide at surface. Cu mesh was then washed with acetone and DI water to remove the residues and cleaned mesh

was dried by blowing with nitrogen flow. In the experiment, 15 mg 2,2'-bipyridine was added in the reacting chamber to improve the selectivity of HCOOH production

Characterizations. X-ray diffraction (XRD) measurements was conducted by A Bruker D8 Advance diffractometer with Cu K α radiation to determine the crystal form of photoelectrodes. X-ray photoelectron spectroscopy (XPS) was obtained by Thermo ESCALAB250 instrument with a monochromatized Al K α line source (200 W), and the UPS data was collected by Thermo ESCALAB 250Xi with He-I α source, which was used to determine the Fermi level and conduction band of the samples. The ultraviolet visible diffuse reflectance spectra (UV-Vis DRS) were conducted by a Varian Cary 500 Scan UV-vis spectrophotometer with barium sulfate as the reference. The time-resolved photoluminescence (PL) spectra were recorded on Hitachi F-7000 FL spectrophotometer. HITACHI SU8010 field emission scanning electron microscopy (SEM) was utilized to investigate the morphologies of the samples, Transmission electron microscopy (TEM) and energy dispersive X-ray spectroscopy (EDX) were performed on a FEI Tencai 20 microscope to study the morphology. The samples for TEM were prepared by peeling the samples from the FTO glasses and suspended in the pure ethanol. Electrochemical tests were performed using a BioLogic VSP-300 electrochemical system and a 50W LED of 395 nm is used as the light source and the input energy of LED light was received by spectrometers (International light, ILT950). The evolved gas was analyzed by a gas chromatograph (Agilent 7820A) equipped with a thermal conductive detector. The 5A molecular sieve column was used as chromatographic column and using Ar ($\geq 99.999\%$) as the carrier gas. NMR spectrum was measured on a Bruker Avance spectrometer for characterizing the liquid production and ion chromatography (Thermoscientific ICS-1100) was utilized to quantitatively analyze liquid products.

Photoelectrochemical CO₂ reduction reaction: The PEC reactor consists of two compartments separated by a piece of Nafion-115 proton exchange membrane. The light window on the reactor was quartz glass so that all the light can be penetrated into it. 0.5 M potassium bicarbonate solution was used as the electrolyte. After adding 2,2'-

bpy to the catholyte, CO₂ gas was purged into the system for 30 minutes before the reaction starts to remove air and achieve CO₂ saturation. We used TCN/TiO₂ photoanode as the working electrode (WE) under illumination, Cu mesh electrode as the counter electrode (CE) and saturated Ag/AgCl as reference electrode (RE), respectively for this PEC CO₂ reduction.

Analysis of CO₂ reduction products. Nuclear magnetic resonance (NMR) was used to characterize the liquid product and we detected that the liquid product was only HCOOH (Figure. S17). Ion chromatography was acquired to qualitatively analyze HCOOH. Gas chromatography is acquired to analyze H₂ evolution.

The order of magnitude of surface Cu atoms is estimated from the size of copper counter electrode and the Cu crystal with face-centered cubic (FCC) structure. The size of the copper counter electrode is 10 mm × 10 mm × 0.11 mm and the lattice parameter of a, which is shown in Figure S19, is 3.613Å. Therefore, the molar mass of surface Cu atoms is calculated as follows:

$$\begin{aligned} n_{Cu} &= \left(\frac{0.01 \times 10^{10}}{1.8065} \times \frac{0.01 \times 10^{10}}{3.613} \times 2 + \frac{0.00011 \times 10^{10}}{1.8065} \times \frac{0.01 \times 10^{10}}{3.613} \times 3 \right) / 6.02 \times 10^{23} \\ &= 0.0051741 \mu mol \end{aligned}$$

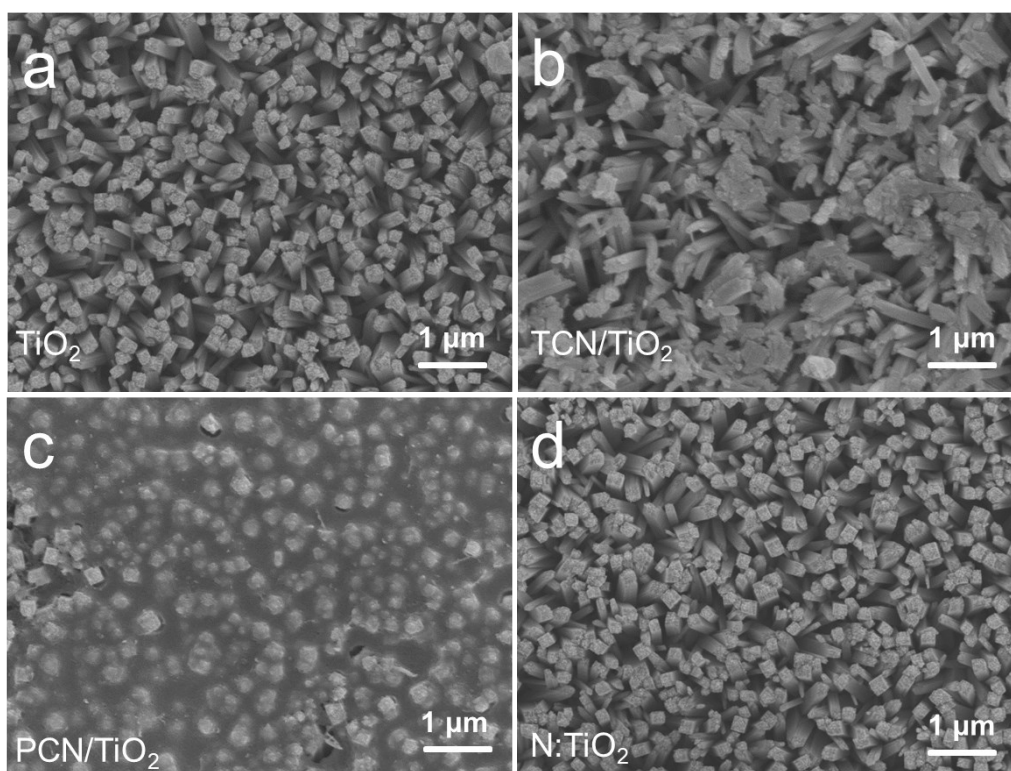


Figure S1. SEM images of (a) TiO₂ nanorods, (b) TCN/TiO₂, (c) PCN/TiO₂ and (d) N:TiO₂ nanorods. They are prepared as photoanodes for oxygen evolution reaction.

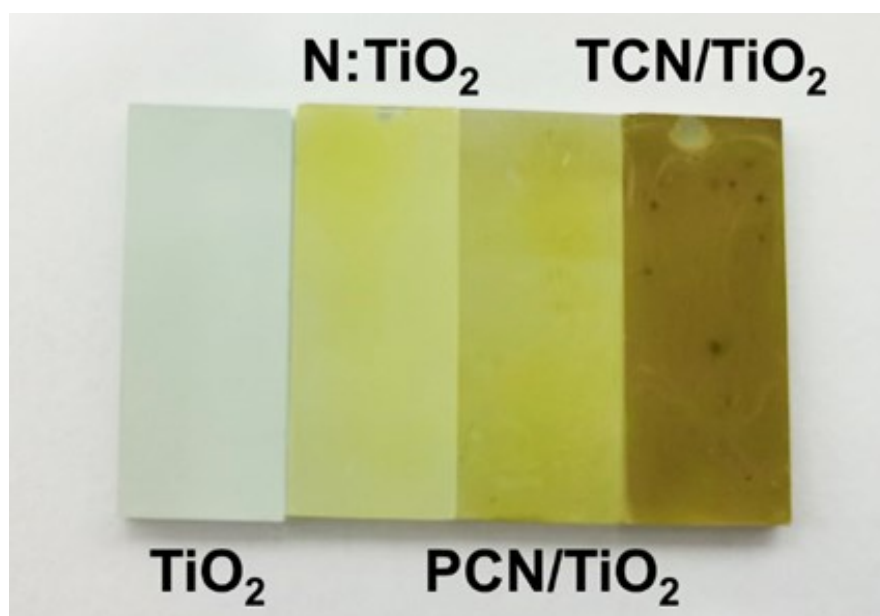


Figure S2. Digital photographs of TiO₂ nanorods, N:TiO₂ nanorods, PCN/TiO₂ and TCN/TiO₂.

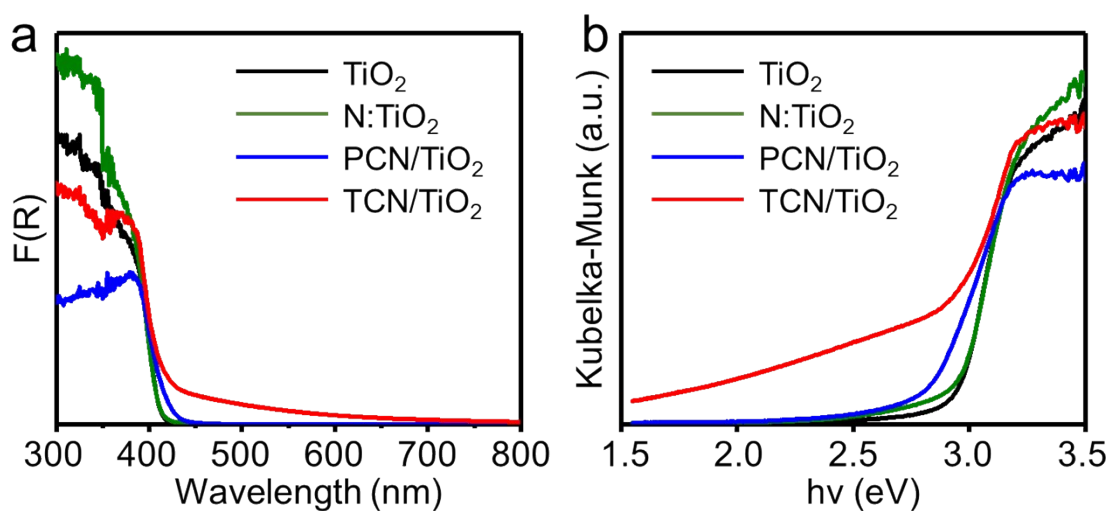


Figure S3. (a) The UV-DRS spectra of the photoanodes and (b) the corresponding Kubelka-Munk plots.

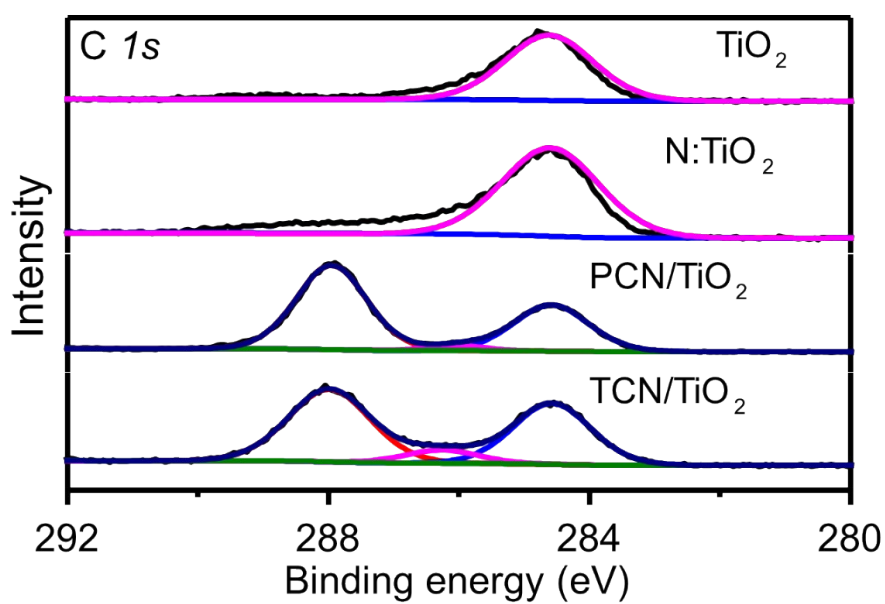


Figure S4. High-resolution $\text{C } 1s$ XPS spectra of photoanodes.

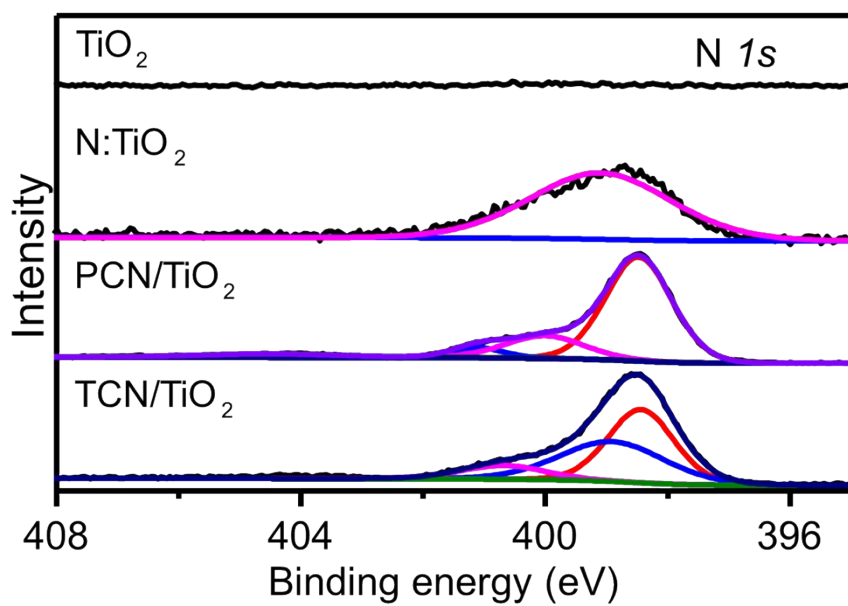


Figure S5. High-resolution N1s XPS spectra of photoanodes.

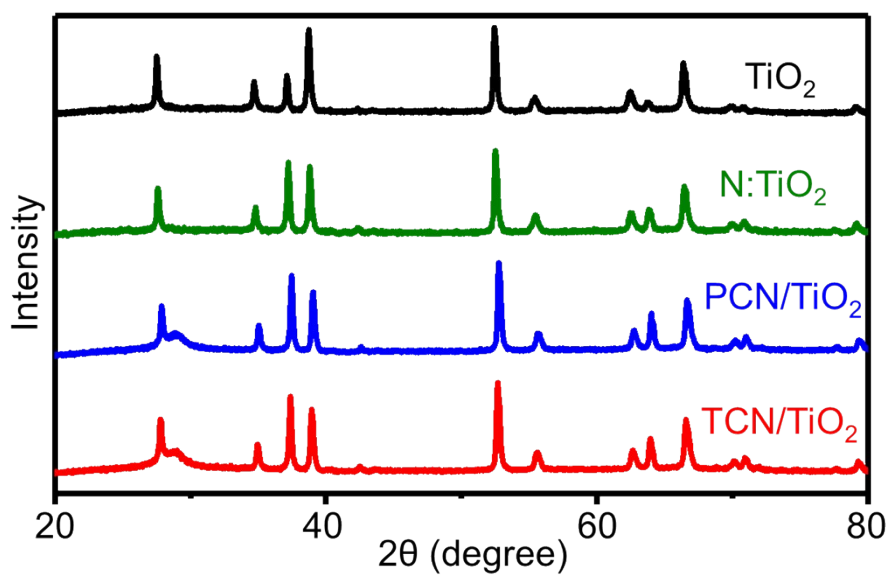


Figure S6. The XRD spectra of the photoanodes.

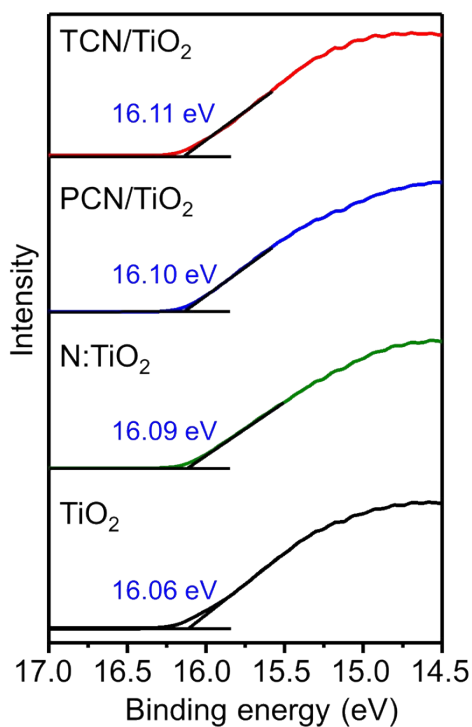


Figure S7. UPS cutting edges of the photoanodes.

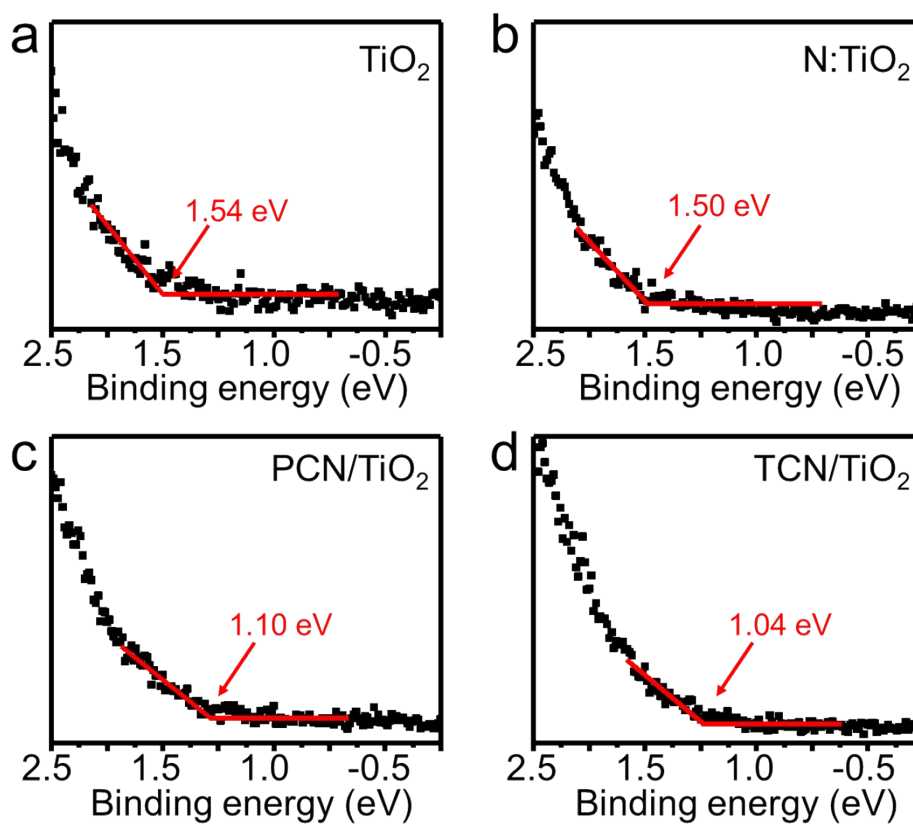


Figure S8. The linear fitting of the UPS Fermi tail of photoanodes to calculate the distance from Fermi level to valence band.

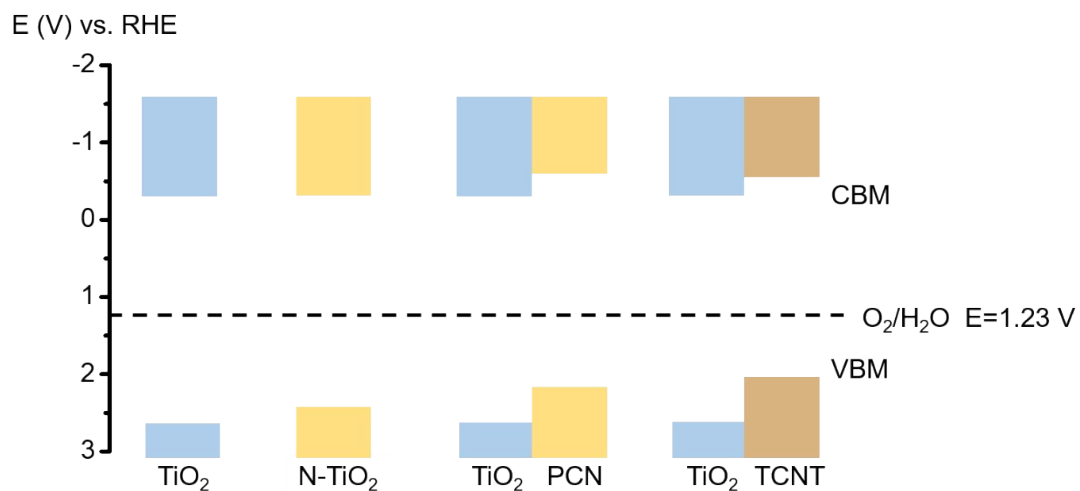


Figure S9. The band structure of TiO_2 , and N-TiO_2 nanorods, and the band alignment by coating PCN and TCN on TiO_2 nanorod arrays.

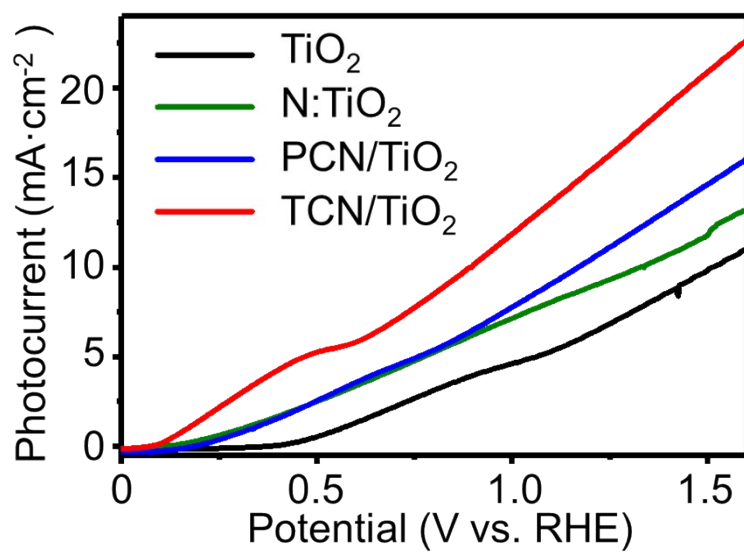


Figure S10. The linear sweep voltammograms curves of the photoanodes.

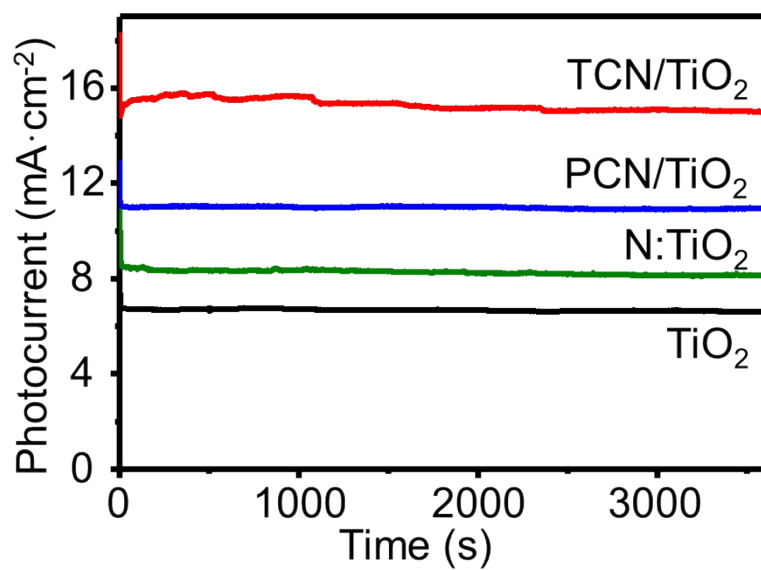


Figure S11. Photocurrent density for the photoanodes at the applied voltage bias of $1.2 V_{\text{RHE}}$.

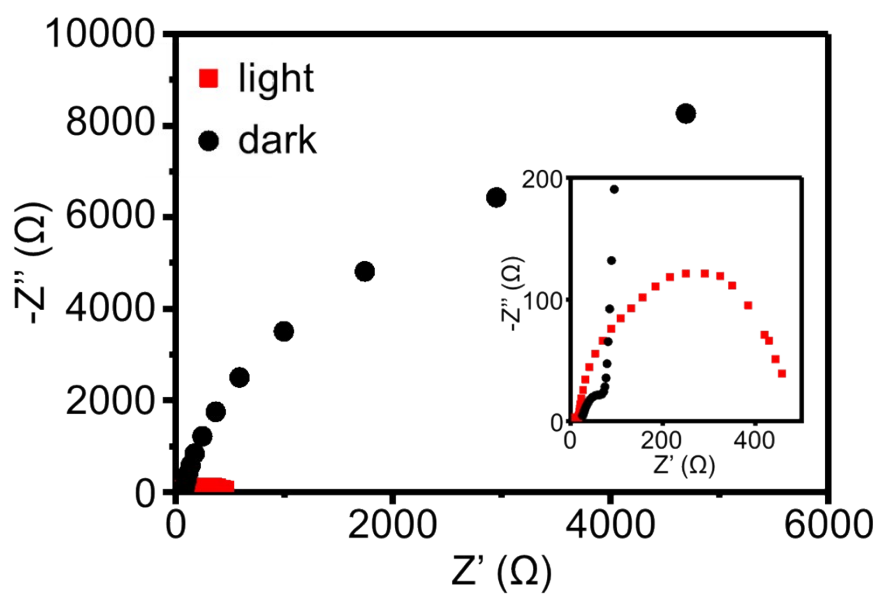


Figure S12. Nyquist plots of the TCN hybrid photoanode with light on and off.

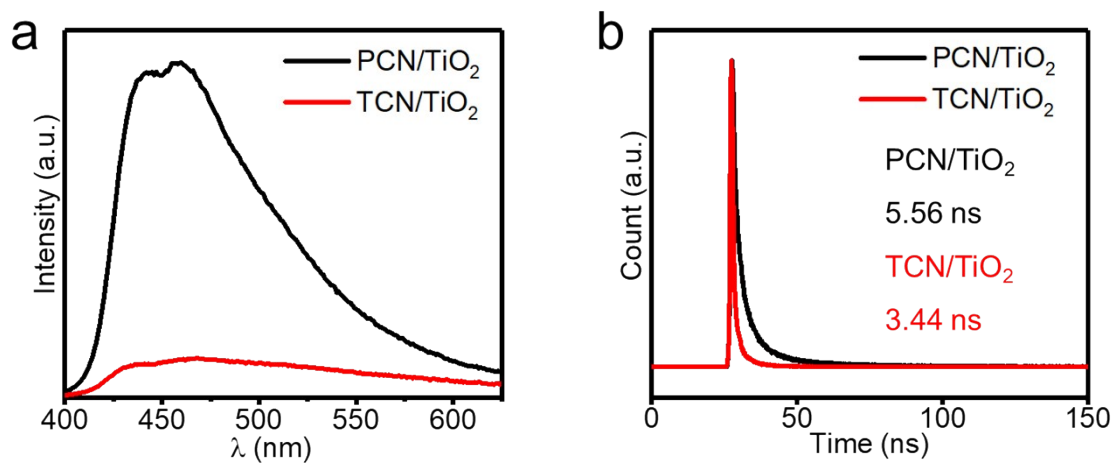


Figure S13. (a) PL spectra of the hybrid photoanodes under 360 nm excitation. (b) Time-resolved photoluminescent spectra of the hybrid photoanodes.

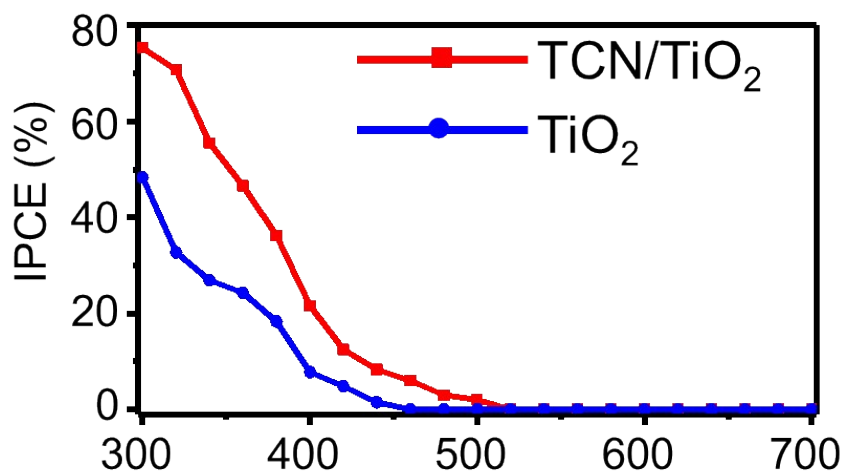


Figure S14. IPCE of TCN/TiO₂ and TiO₂ photoanodes.

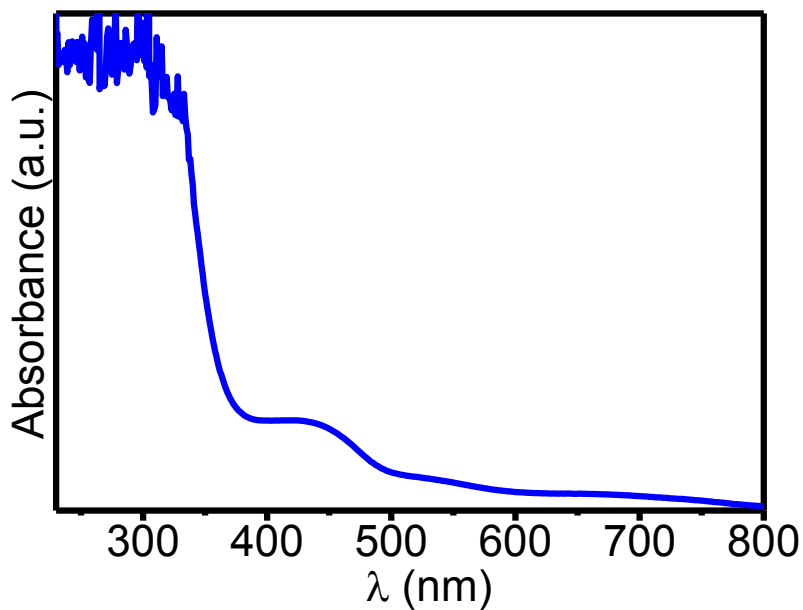


Figure S15. UV/Vis spectra of Cu mesh in 2,2'-bipyridine abundant electrolyte solution with purging of CO₂ gas.

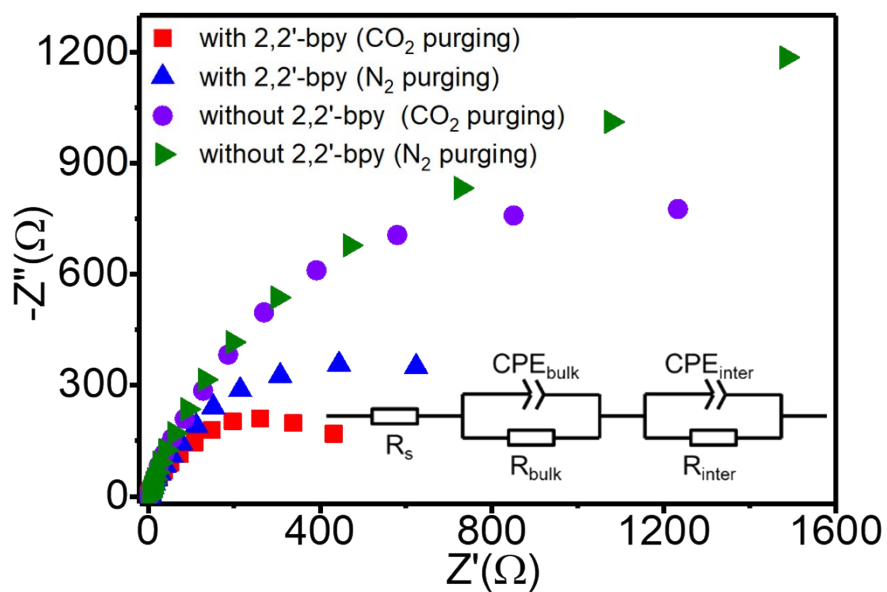


Figure S16. Nyquist plots of Cu cathode with controlled conductions in 0.5 M KHCO₃ solution and equivalent circuit.

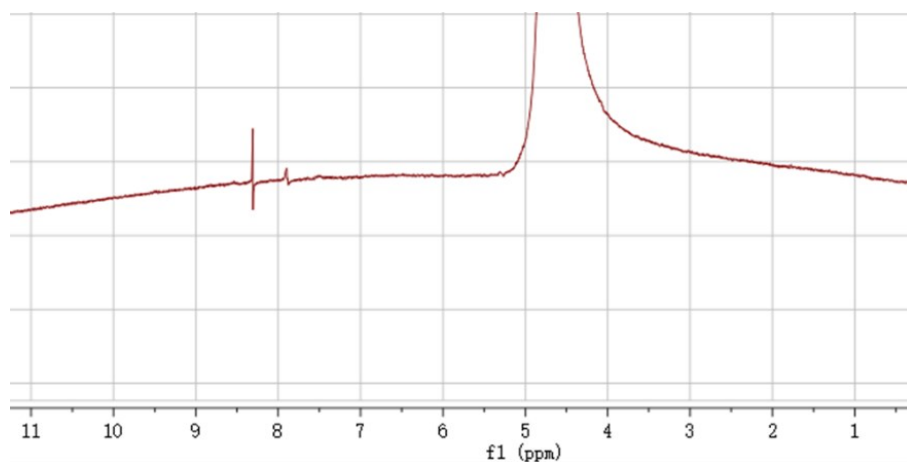


Figure S17. NMR spectra of the electrolyte to probe product. The signal peak near 8.5ppm indicates the formation of HCOOH. The weak signal peak near 7.8ppm is 2,2'-bipyridine in the electrolyte as it is slightly soluble in aqueous electrolyte solution.

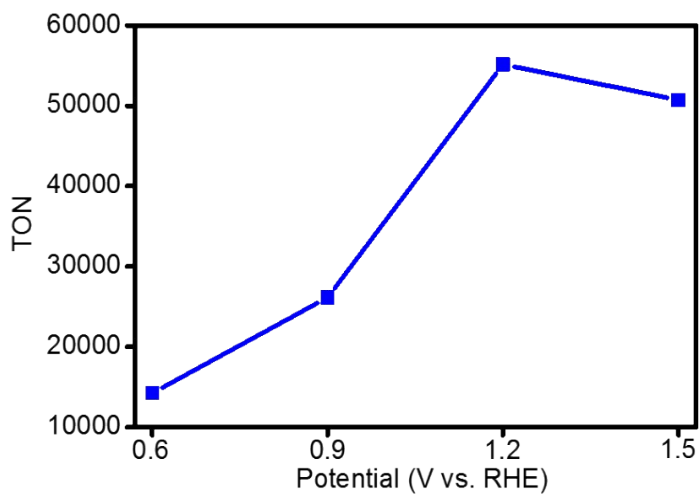


Figure S18. Turnover numbers for HCOOH was calculated after 3 hours.

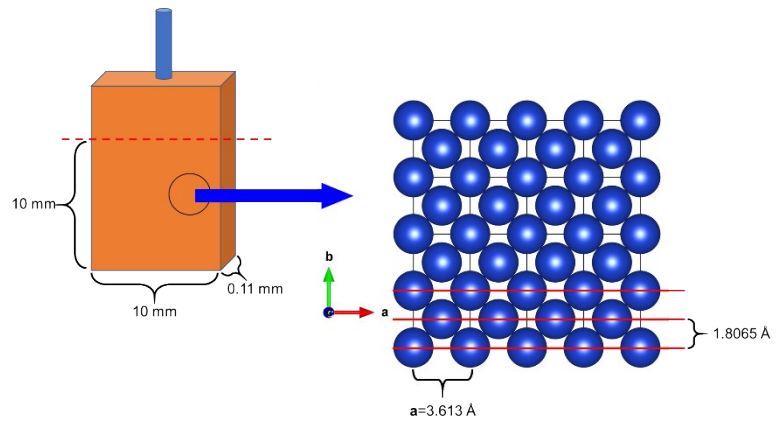


Figure S19. The estimation of the order of magnitude of the surface Cu atoms based on the Cu crystal with FCC structure.

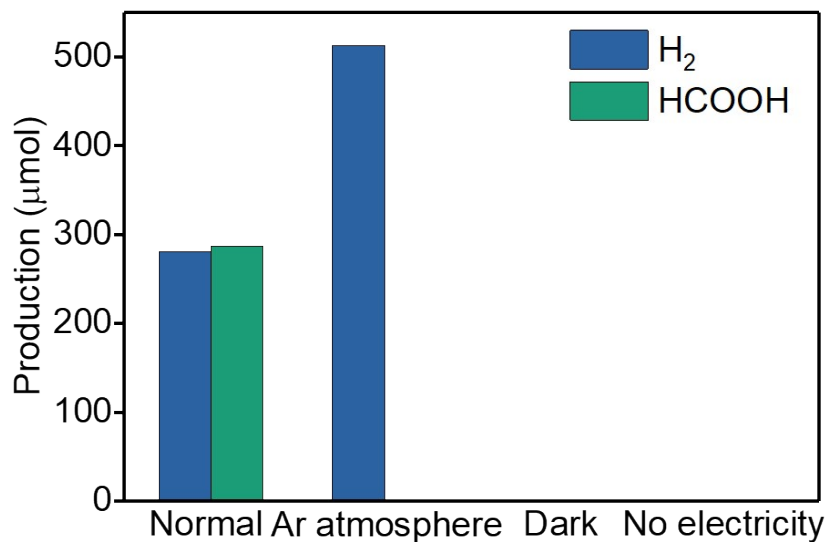
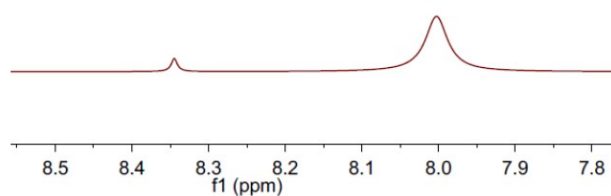


Figure S20. The reference experiments with different reaction conditions. H₂ gas was obtained as the product when using Ar as purging gas, and we cannot obtain any results without either light or electric support.

(a)



(b)

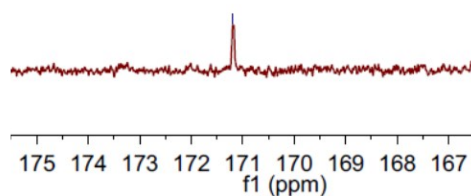


Figure S21. (a) ¹H-NMR spectrum and (b) ¹³C-NMR spectrum of products for ¹³CO₂ labelling experiments.

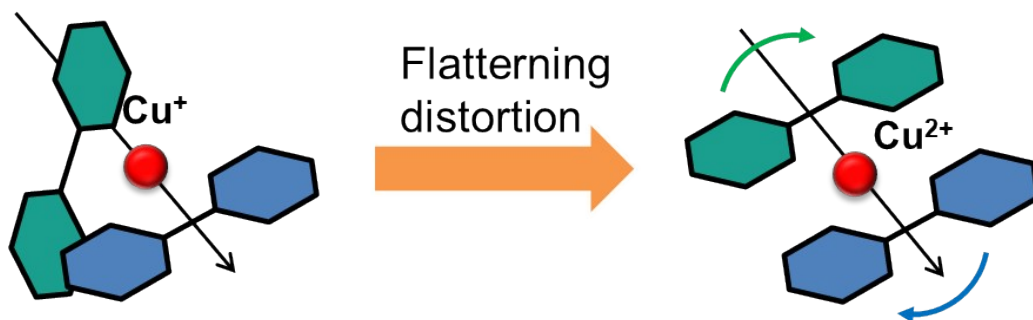


Figure S22. Flattening distortion when Cu coordinates with 2,2'-bipyridine.

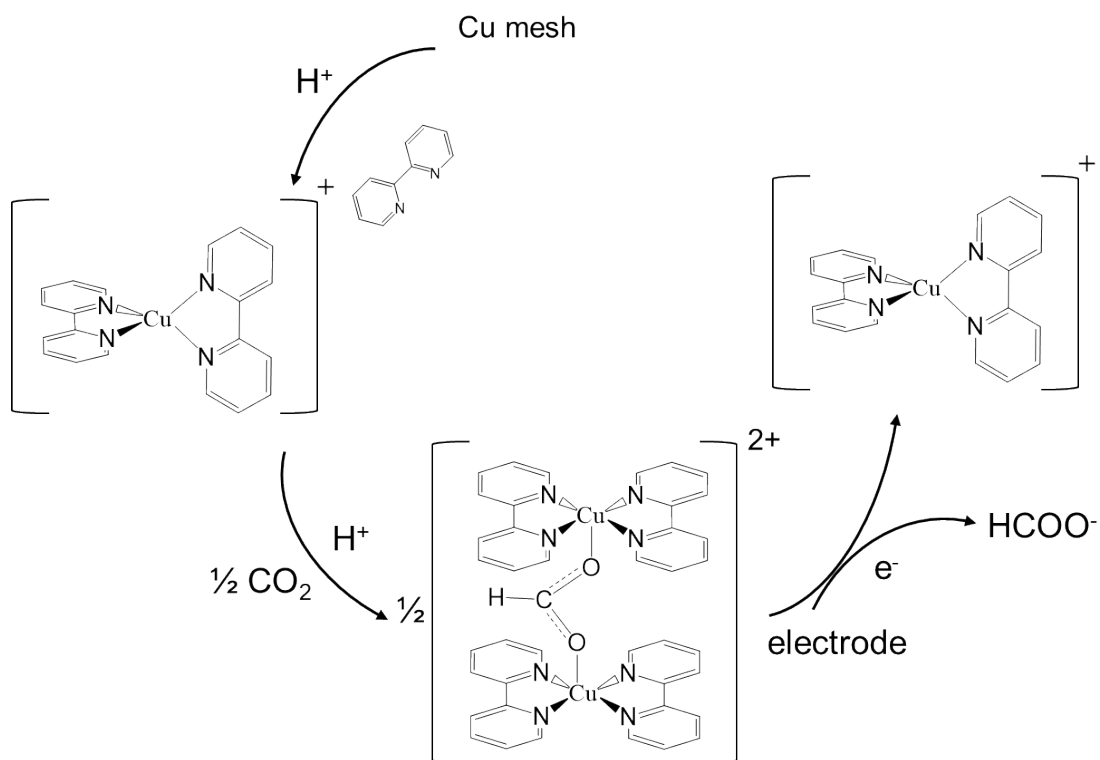


Figure S23. The possible mechanism to immobilize CO_2 and form HCOO^- by the Cu cathode with abundant of 2,2'-bipyridine in the electrolyte solution.

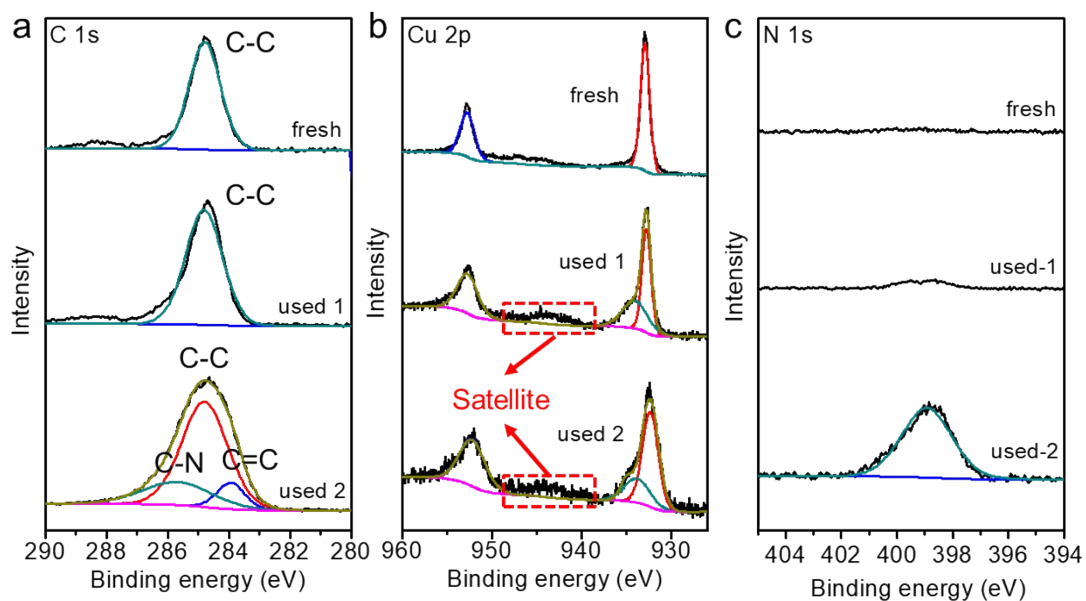


Figure S24. (a) C 1s, (b) Cu 2p, and (c) N 1s XPS spectra of the fresh copper mesh and used Cu mesh to prove the coordination structure between Cu and 2,2'-bipyridine. (used 1 is the sample after CO₂ reduction without adding 2,2'-bipyridine and used 2 is the sample after CO₂ reduction with adding 2,2'-bipyridine.)

Table S1. The band structures of the photoanodic materials.

Material	Fermi level (V vs.RHE pH=0)	VB (V vs.RHE pH=0)	CB (V vs RHE. pH=0)
TiO ₂	0.64	2.60	-0.37
N:TiO ₂	0.62	2.54	-0.36
PCN	0.60	2.11	-0.67
TCN	0.58	2.03	-0.65

Table S2. Fitted parameters for EIS results of Figure S15.

Electrolyte	R _s	R _{bulk}	CPE _{bulk}	R _{inter}	CPE _{inter}
With 2,2'- bipyridine (CO ₂ purging)	1.513	33.63	1.544×10 ⁻⁴	541.3	2.874×10 ⁻⁴
With 2,2'- bipyridine (N ₂ purging)	1.533	35.76	1.404×10 ⁻⁴	941.4	2.428×10 ⁻⁴
Without 2,2'- bipyridine (CO ₂ purging)	1.536	37.13	1.508×10 ⁻⁴	1750	2.603×10 ⁻⁴
Without 2,2'- bipyridine (N ₂ purging)	1.516	35.13	1.638×10 ⁻⁴	1895	2.238×10 ⁻⁴